Enabling High Data Rate VLC via MIMO-LEDs PPM

Mauro Biagi[♮], and Anna Maria Vegni[♯]
[♮]Department of Information, Electronics and Telecommunication, University of Rome "Sapienza",
Rome, Italy, *mauro.biagi@uniroma1.it*
[♯]Department of Engineering, University of Roma Tre,
Rome, Italy, *annamaria.vegni@uniroma3.it*

***Abstract*—Visible light communication is a new frontier of communication allowing high data-rate Internet access specially in indoor environment. One of the key challenges is the limited modulation bandwidth of sources, that is typically around several MHz. As a room or coverage space would typically be illuminated by an array of Light Emitting Diode devices, there exists the potential for parallel data transmission.**

In this paper we investigate the use of multiple LEDs to perform a space-time block coding. By exploiting optical MIMO techniques, jointly with Pulse Position Modulation, we can achieve data rates of the order of hundreds of Mb/s (*i.e.*, around 600 Mb/s) in indoor VLC systems, with no reduction of link reliability. Finally, the proposed approach has been compared to similar techniques, highlighting its effectiveness and robustness.

I. Introduction

Recently, the scientific community has paid a lot of attention to Visible Light Communications (VLC) systems, since the idea of using the same light source for illumination and for providing wireless connectivity may allow a more flexible way to access the Internet, and makes simple hardware installation, [1], [2]. In this "dual-use" paradigm, VLC offers several advantages that make it a great complement to the well-established Radio-Frequency (RF) communications. Among the main advantages belonging to VLC, we cite (*i*) the free use of the visible light spectrum, (*ii*) the directional of optical transmissions, and (*iii*) the secure indoor transmission, allowing coexistence of many non-interfering links in close proximity. All these features enable greater data rate densities (Mbit/s/m^2) [3], as well as improved security, compared to traditional RF systems.

In case of real optical channels, multipath effect can largely affect performance. Several approaches for avoiding signal distortion have been discussed in the literature, mostly based on multi-carrier modulation schemes [4], as well as bandwidth-efficient encoding schemes. As an instance, Pulse Amplitude Modulation and Quadrature Amplitude Modulation, are used to increase data rate, assuming that a higher requirement for signal power is met. These can be combined with Discrete Multi-Tone (DMT) modulation to reach data rates of $800+$ Mbit/s in the lab [5], [6]. As a drawback, bandwidth-efficient modulation schemes, and multi-carrier schemes such as DMT, have a distinct disadvantage from the all-important perspective of satisfying the lighting mission [7]. This strongly motivates the use of wideband *on-off* schemes, such as Non-Return-to-Zero or Pulse Position Modulation (PPM) for VLC.

The possibility of using Multiple Input Multiple Output (MIMO) transmission/reception schemes has been already introduced in [8], considering a MIMO-LED scheme based on imaging with 4 LEDs and 4 photodiodes. Also in [9], MIMO approach has been assumed, by evaluating performance of different modulation schemes under the hypotheses of alignment and unaligned between LEDs and photodiodes.

In this paper, we propose a MIMO-LEDs architecture with the assumption of using Space-Time Block Coding (STBC) based on PPM, in order to increase the transmission rate without inducing signal degradation. Under such assumption, the MIMO-LEDs scheme can be represented via the use of vectors and matrices. This modulation format is sufficiently simple to implement and allows the space-time matrix to have some interesting properties and, more, PPM can be used also for localization purposes (see [10]). Finally, some impairments have been considered as the effect of imperfect channel knowledge, channel delay spread and also the effect of spatial correlation.

The remainder of this paper is organized as follows. Section II gives background on existing VLC approaches for indoor wireless communications, including a description of the relevant characteristics of the channel model. In Section III, we define the proposed MIMO-LEDs architecture based on PPM-STBC technique, which will be illustrated in more detail in Section III-A. Considerations on modeling of receiver architecture are then given in Section III-B. In Section IV, numerical results are expressed in terms of Bit Error Rate and achievable data rates; also, a comparison to other techniques has been carried out. Finally, conclusions are drawn at the end of the paper.

II. Indoor Optical Wireless Communication Essentials

All optical wireless communications, including VLC, use intensity modulation and direct detection (IM/DD). Let us consider the mostly generalized case of an optical channel, in which a desired transmitted optical intensity waveform $X(t)$ of T_p time duration arrives at a photodiode receiver. It will produce an electrical current $Y(t)$, proportional to $X(t)$, whose expression is:

$$Y(t) = rA_e X(t) * h(t) + W(t), \tag{1}$$

where r [A/W] is the responsivity of the photodiode, A_e [m^2] is the effective receiver area, $h(t)$ is the channel impulse response, and $W(t)$ is the shot noise due to ambient light, nominally Poisson distributed. Eq. (1) is a simplified representation of output signal in an optical channel, and hides much detail, which our modeling does take into account [11]. For example, A_e depends on the actual photodiode area, the angle of light incidence, and the concentrator used [12], [13].

For sufficiently low rates R_b [bit/s], $h(t)$ can be approximated to H_0 [m^{-2}] that is the DC gain of an ideal channel, while for higher rates, the signal distortion becomes important and not negligible, since it may cause inter-pulse (and/or inter-symbol) interference. In the case, a very good short-hand predictor of optical link performance in the presence of distortion is the r.m.s. delay spread of the response $h(t)$. Namely, it must be short compared to the symbol time (*i.e.*, $T = R_b^{-1}$), in order to avoid significant effects from Inter-Symbol Interference, [14].

For what concerns the channel modeling, we distinguish between "white" and "blue" channel, respectively with channel impulse responses $h_w(t)$ and $h_b(t)$. The first term $h_w(t)$ includes distortions introduced by (*i*) the white LED (*i.e.*, $g_w(t)$), (*ii*) the free-space signal propagation, including multipath (*i.e.*, $g_f(t)$), and (*iii*) the receiver (*i.e.*, $g_r(t)$), as follows:

$$h_w(t) = g_w(t) * g_f(t) * g_r(t). \tag{2}$$

As early mentioned, we consider "white" LEDs optimized for illumination, not yet for communications; as a result, the choice of design parameters is very limited. Indeed, currently available "white" LEDs are constructed from a ≈ 450 nm "blue" LED chip encased in a phosphor material that converts blue light to a broad spectrum yellow. The combination of the blue light that escapes unchanged and the yellow phosphor light appears white to humans. Only the blue component is modulated directly, while the yellow one responds to blue pulses with a delay and a longer phosphorescence effect. This is mathematically expressed by means of the following "white" LED impulse response, as a combination of multiple terms:

$$g_w(t) = g_b(t) + g_y(t), \tag{3}$$

where $g_b(t)$ and $g_y(t)$ are respectively the blue and yellow portions of "white" LED response $g_w(t)$, corresponding to a 3-dB modulation bandwidth of ~ 2 MHz. The blue portion $g_b(t)$ intrinsically may have a 3-dB bandwidth up to ~ 20 MHz, which can be accessed by removing the yellow contribution by using a 450 nm bandpass optical filter placed in front of the receiver. This allows us to represent the "blue" channel impulse response as:

$$h_b(t) = g_b(t) * g_f(t) * g_r(t), \tag{4}$$

which implies a lower received signal power in blue range than the white, mainly due to removing g_y that is the slower modulated signal emitted by the phosphor at longer color wavelengths.[1]

[1]Notice that this filter also reduces shot noise by rejecting DC ambient light in the environment at those wavelengths.

In our model we will use the approximated response for a "white" Luxeon Star LED, as measured in [15], which is quite representative of other LEDs. The fit for the blue-only channel is $G_b(\omega) = e^{-\omega/\omega_1}$, with $\omega_1 = 2\pi \times 15.5 \times 10^6$ rad/s. This approximation gives $g_b(t)$ with a r.m.s. delay spread of 10.2 ns. For the "white" modulation response, it can be approximated similarly as:

$$G_w(\omega) = \begin{cases} e^{-\omega/\omega_2} & \text{if } \omega < \omega_c \\ e^{-\omega_c/\omega_2} \cdot e^{\omega_c/\omega_3} \cdot e^{-\omega/\omega_3} & \text{if } \omega > \omega_c \end{cases} \tag{5}$$

where $\omega_2 = 2\pi \times 3.26 \times 10^6$, $\omega_3 = 2\pi \times 10.86 \times 10^6$ and $\omega_c = 2\pi \times 10^6$ rad/s. The corresponding delay spread is 47.5 ns. The free-space channel $g_f(t)$ has a relatively smaller delay spread, though it depends on whether the link is (*i*) directed or diffuse, (*ii*) LOS or NLOS (shadowed), as well as on (*iii*) the environmental conditions (*i.e.*, distance from the receiver, room size, and surface reflectivities). Leveraging on those considerations, we can distinguish three basic cases for channel modeling:

1) *Pure LOS channel* (*pLOS*), with a DC attenuation H but negligible multipath component, *i.e.* $g_f(t) \approx H\delta(t)$. This type of channel occurs with short distance LOS links (around tens of centimeters), [15];
2) *Medium range LOS channel* (*mLOS*), with LOS component but also significant delayed components due to reflected secondary paths. The energy is spread over the time, resulting in a reduction of the converted current at the photodiode. This scenario well matches with a transmission at $1 - 2$ meters so the diversity gain is expected to be higher than that of *pLOS*;
3) *NLOS channel* (*NLOS*), with no LOS paths due to shadowing. The link relies on collecting only the reflected paths, leading to inter-symbol and inter-pulse interference. Moreover, pulse overlapping can occur if the PPM transmission rate is higher with respect to the reciprocal of channel delay spread. The diversity gain is then expected to be high, and in the case of very high PPM rate for single LED scenario, equalization is required. However, in the proposed MIMO-LED approach, no equalization is expected since our technique can increase rate without stressing the time domain.

Finally, a receiver can be chosen to greatly outperform the LED and the channel in terms of bandwidth, as in [15] where a 15 mm^2 active area PIN receiver with a 77 MHz bandwidth has been used. Therefore, we can assume $g_r(t) = \delta(t)$.

III. Proposed technique

This section introduces the proposed architecture relying on MIMO technique for VLC applications. The main aspects (*i.e.*, channel modeling at the transmitter side for three different cases) are investigated, while STBC and PPM approaches are described in Subsection III-A. Finally, the received architecture is discussed in Subsection III-B.

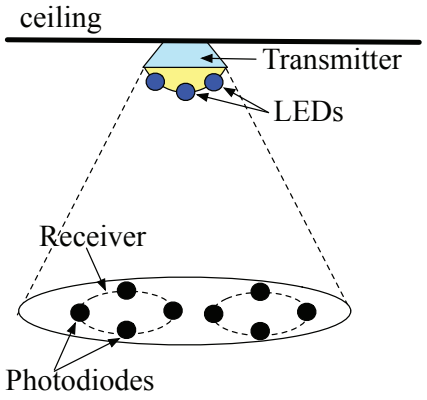

Fig. 1. Scheme of indoor MIMO-LEDs. The transmitter (receiver) is comprised of n_T (n_R) LEDs (photodiodes).

The MIMO-LEDs scheme can be represented via the use of vectors and matrices. Let us start from a model where the channel is flat with respect to the frequency response (*i.e.*, LOS scenario). We assume $n_{T,R}$ as the number of LEDs and photodiodes at the transmitter and the receiver sides, respectively. Fig. 1 describes the considered scheme in an indoor environment.

The received signal can be written in the following way

$$\mathbf{Y} = \mathbf{XH} + \mathbf{W}, \tag{6}$$

where $\mathbf{Y}$ is the $[L \times n_R]$ matrix collecting the L-PPM symbols received by the n_R photodiodes. $\mathbf{H}$ is a $[n_T \times n_R]$ matrix, where each element in the position (i, j) is the channel path between the i-th transmitting LED and the j-th receiving photodiode. The term $\mathbf{W}$ is a $[L \times n_R]$ matrix, describing the whole disturbance, expressed in terms of thermal and ambient noise. Last, $\mathbf{X}$ is the STBC $[L \times n_T]$ matrix that carries information according to the cardinality of PPM and the number of transmitting LEDs.

Eq. (6) shows a discrete-time representation of what is present at the receive photodiodes; by fact, each of the n_R photodiodes receives n_T analog signals coming from the n_T transmitting LEDs, and weighted –filtered– by the channels. The corresponding (analog baseband) signal (*i.e.*, $y_j(t)$), measured at the output of the j-th receive photodiode over a signaling period $T_s = T_p + T_g$ (being T_g a guard-time interval), may be expressed in its general form as

$$y_j(t) = \frac{1}{\sqrt{n_T}} \sum_{i=1}^{n_T} h_{ji}(t) \cdot X^{(i)}(t) + W_j(t) =$$

$$= \frac{1}{\sqrt{n_T}} \sum_{i=1}^{n_T} \left[\sum_{n=0}^{V} h_n(j,i) X^{(i)}(t - \tau_n(j,i)) \right] + W_j(t),$$

$$0 \le t \le T_s,\ 1 \le j \le n_R, \tag{7}$$

where $w_j(t)$ are the noise components at each receive photodiode, while $h_n(j,i)$ is the amplitude of one out of $(V+1)$ paths associated to the $\tau_n(j,i)$ delay related to the link between the i-th LED and the j-th photodiode. Moving from $y_j(t)$ to $\mathbf{y}_j(n)$ can be obtained by sampling the output at the pulse period T_p, as

$$\mathbf{y}_j(n) = y_j(t)\big|_{t=\left[\frac{T_p}{2} + nT_p\right]},\ \ 0 \le n \le L-1. \tag{8}$$

A. Space-Time PPM Block Coding

The matrix $\mathbf{X}$ logically describes the presence of a pulse among the time axis and on the space (due to the LEDs deployment). By assuming a $(L = 2)$-PPM performed over $(n_T = 2)$ LEDs, the matrix dimension is then 2×2. As well known from the literature and as it will appear clear in the following, PPM is bandwidth inefficient, while it is power efficient. The way to counterbalance the inefficiency in terms of bandwidth (*i.e.*, rate), is to use spatial diversity. The maximum allowed number of matrix is L^{n_T}, under the constraint of transmitting only one signal per slot by each slot; in matrix form this means to have a sole 1 on each matrix column, such as

$$\mathbf{C}_1 = \begin{bmatrix} 1 & 0 \\ 0 & 1 \end{bmatrix}, \mathbf{C}_2 = \begin{bmatrix} 0 & 1 \\ 1 & 0 \end{bmatrix},$$

$$\mathbf{C}_3 = \begin{bmatrix} 1 & 1 \\ 0 & 0 \end{bmatrix}, \mathbf{C}_4 = \begin{bmatrix} 0 & 0 \\ 1 & 1 \end{bmatrix}. \tag{9}$$

Considering the matrix $\mathbf{C}_1$ in the $[2\times2]$ model, since the generic i-th column represents the signal emitted by the i-th LED (with $1 \le i \le n_T$), we name as $C_1^{(1)}(t)$ the analog signal emitted by the first LED, while $C_1^{(2)}(t)$ represents the signal emitted by the second one. They are expressed as follows

$$C_1^{(1)}(t) = \frac{1}{\sqrt{n_T}} X(t) \quad \text{and} \quad C_1^{(2)}(t) = \frac{1}{\sqrt{n_T}} X(t - \Delta), \tag{10}$$

being Δ the PPM time-shift.

By using only matrices $\mathbf{C}_1$ and $\mathbf{C}_2$ [2], it is possible to achieve an orthogonal space-time block coding. This allows to use only 2 codewords, while the simultaneous use of 4 codewords allows to achieve twice the data rate. By assuming the pulse duration equal to T_p and a guard time T_g, the time length of each column is $L \cdot T_s$. Thus, the total rate is

$$R = \frac{1}{L \cdot T_s} \log_2(L^{n_T}), \tag{11}$$

which in the case of $n_T = n_R = 2$ and $L = 2$ becomes $R = T_s^{-1}$, while for a single LED link (*i.e.*, $n_T = n_R = 1$) the data rate is $R = 0.5 \cdot T_s^{-1}$. An increase of L without reducing T_s decreases the value of R, while an increase of the number of LEDs/photodiodes rises the rate. So, the achievement of high rate values is due to both the possibility of having several LEDs/photodiodes, that can be installed also in small rooms, and the LED ability to quickly operate the electrical-to-optical conversion.

In the more general case of n_T transmitting LEDs and L-PPM modulation, the number of possible matrix codewords is L^{n_T} and the z-th matrix (with $z \le L^{n_T} \in \mathbb{R}^+$) is given by

$$\mathbf{C}_z = \left[\mathbf{e}_z^{(1)}\ \mathbf{e}_z^{(2)}\ \cdots\ \mathbf{e}_z^{(i)}\ \cdots\ \mathbf{e}_z^{(n_T-1)}\ \mathbf{e}_z^{(n_T)} \right], \tag{12}$$

where the i-th element $\mathbf{e}_z^{(i)}$, associated to the i-th LED, is a $[1 \times L]$ column vector constituted by all zeros and only one 1. Again, this is the discrete-time representation of the matrix, related to the analog signals transmitted by LEDs.

[2] The same happens by choosing only $\mathbf{C}_3$ and $\mathbf{C}_4$.

B. Receiver Architecture

The channel knowledge at the receiver is fundamental to perform a correct detection/decoding process. It is reasonable to assume that some pilot pulses may be transmitted, allowing the receiver to acquire sufficient information about the propagation environment. From (9), the following property holds:

$$\mathrm{Tr}\{\mathbf{C}_l^T \mathbf{C}_m\} \leq 2, \tag{13}$$

where the equality occurs if, and only if, $l = m$. So, a receiver based on the maximum trace may assure the correct detection. For a general matrix dimension, as a general codeword, the following relationship holds

$$\mathrm{Tr}\{\mathbf{C}_l^T \mathbf{C}_m\} \leq n_T, \tag{14}$$

and again, the equality holds if $l = m$. Unfortunately, the presence of the channel mixes the spatial components; even in the absence of noise, the trace properties of the matrices in (13) and (14) are altered due to channel. This suggests to spatially *solve the channel* by inverting it via a matrix inversion operation (in the case of squared matrix) or via the use of a pseudo-inverse matrix (used for rectangular matrix). After the optical-to-electrical conversion operated by the photodiode, the received matrix $\mathbf{Y}$ should be processed in order to obtain a decision variable (*i.e.*, $\mathbf{Z}$) defined as follows

$$\mathbf{Z} = \mathbf{Y}\mathbf{H}^{\sharp} = \mathbf{X} + \mathbf{W}\mathbf{H}^{\sharp}, \tag{15}$$

where the symbol $^{\sharp}$ means (*i*) inversion or (*ii*) pseudo-inversion operation, depending on the matrix dimension *i.e.*, (*i*) squared or (*ii*) rectangular, respectively. Once obtained the decision variable $\mathbf{Z}$, the decided codeword will be

$$\hat{\mathbf{C}}_i = \arg\max_i \mathrm{Tr}\{\mathbf{C}_i^T \mathbf{Z}\}. \tag{16}$$

This decision mechanism directly comes from (14) and (15). In fact, when the space-filtered noise $\mathbf{W}\mathbf{H}^{\sharp}$ in (15) is negligible, $\mathbf{Z}$ approaches $\mathbf{X}$, so by using the property in (14) we can recognize the transmitted codeword.

To summarize, the main aspects of the receiver are the following: (*i*) it is evident from (15) that the *channel inversion* may increase the level of noise mainly because the channel coefficients of the matrix $\mathbf{H}^{\sharp}$ are usually bigger than unity; (*ii*) when the transmitter and receiver are very close each other –*short-distance communications*–, the inversion may give rise to bad-conditioning and the inversion process may result numerically complicated; (*iii*) in the case of *imperfect* channel knowledge, the inversion is not perfect as well.

IV. Numerical Results

The simulations have been developed under the parameter assumptions collected in TABLE I, with the optimistic assumption of *perfect* channel knowledge. The channel model between each LED and photodiode has been obtained through CandLES simulator, [11]. In the simulations we assumed that the PPM time shift Δ equates $T_s = 12.98 \cdot 10^{-9}$ s.

The simulations have been performed by considering a use case scenario that is an open office at the Department of Applied Electronics of Roma Tre University (see Fig. 2), as previously used in [16] and [10]. Results have been spatially sampled so as to present values averaged over the room positions.

TABLE I. Model Parameters

LED Transmitter	
Maximum transmit sum power (white) P_t	1 W
Beam angle	45° FWHM
Room setup	
Dimensions ($l \times w \times h$)	10 m $\times$9 m $\times$3 m
Surface reflectivities	0.8
Ambient (DC) irradiance	5.8μW/(cm$^2\times$ nm)
Receiver	
FOV	90°
Area	15 mm^2
Lens gain factor	2.2
Effective area A_e	33 mm^2
Optical filter	450 ± 20 nm, 60% through
Responsivity @450 nm	0.2 A/W
Responsivity @650 nm	0.4 A/W

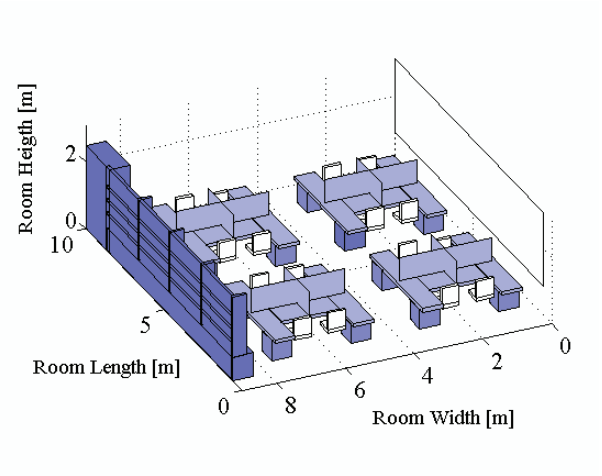

Fig. 2. Scheme of the scenario used in our simulations. The open office is at the Department of Applied Electronics of Roma Tre University.

This scenario is comprised of four workstations with several chairs and has been designed via Candles software. The wall reflectivity is 80%, while for the workspaces it is 50%, as typical as for wooden tables. Under each workspace, there is a chest whose reflectivity has been assumed equal to 70%. No reflectivity factor has been assumed for the chairs. Along the south wall, there is a huge window covering almost the room length, with a reflectivity factor of 0%; while along the north wall, we assume a bookcase with 80% of reflectivity. Four LED transmitters are placed on the ceiling, in positions corresponding to each workstation (*i.e.*, LED_1 is in $P_1 = (2, 4, 3)$, LED_2 in $P_2 = (6, 4, 3)$, LED_3 in $P_3 = (2, 8, 3)$, and LED_4 in $P_4 = (6, 8, 3)$).

Fig. 3 shows the simultaneous effect on achievable rate of the number L of PPM symbols and of the number of LEDs/photodiodes, according to (11). By increasing L from 2 to 64, the value of R decreases from 38.5 Mb/s to 7.21 Mb/s when only one LED/photodiode pair is considered, while for 16 LED/photodiode pairs, the achievable rate falls from 616 Mb/s to 115.5 Mb/s. This suggests that increasing the order of L-PPM modulation is not worth, while increasing the number of LEDs/photodiodes allows to achieve very high rates. The limitation given by the L-PPM order may be fixed

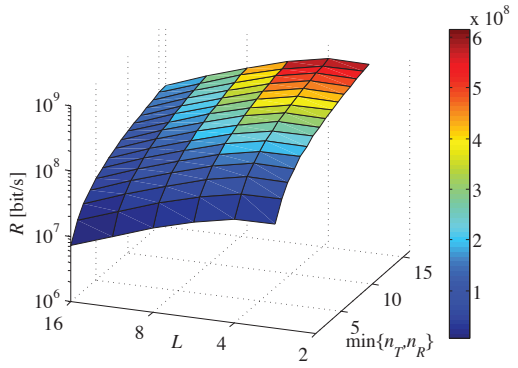

Fig. 3. Achievable rate for different values of L, n_T and n_R.

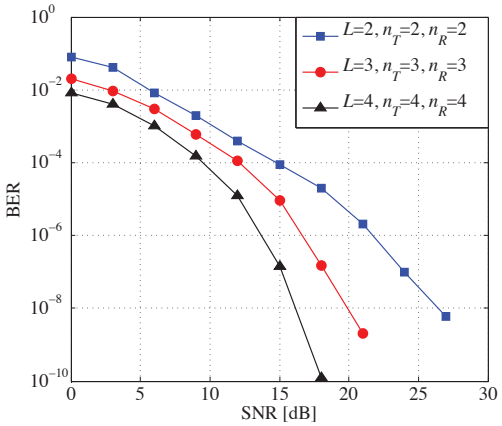

Fig. 4. BER for different values of L, n_T and n_R, vs. SNR.

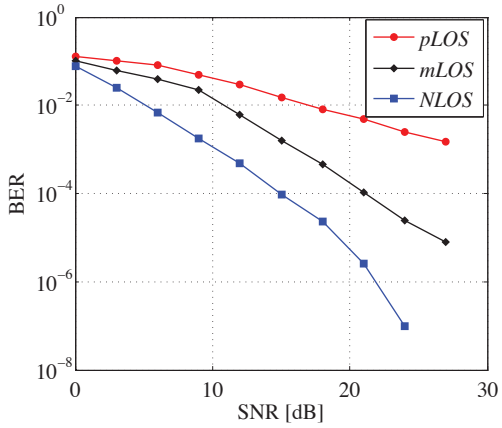

Fig. 5. BER for different propagation scenarios in a $[2 \times 2]$ system with 2-PPM, vs. SNR.

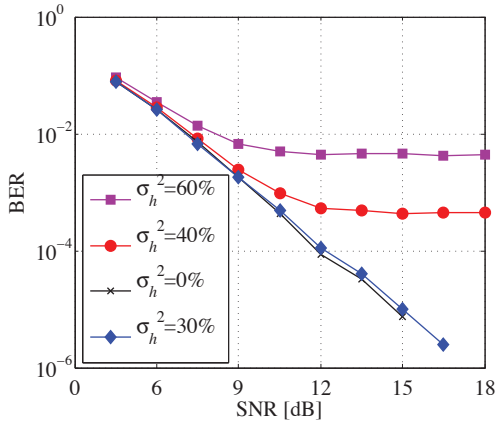

Fig. 6. BER for different levels of estimation error in a $[2 \times 2]$ system with 2-PPM, vs. SNR.

by adapting the T_s value to make the product $(L \cdot T_s)$ in (11) constant. In order to do so, a technological issue should be tackled since, as previously anticipated, this is strictly tied to the ability of LEDs to quickly perform the electrical-to-optical conversion.

Fig. 4 depicts the BER obtained for different values of L, and $n_{T,R}$. Notice how passing from $(L = n_T = n_R = 2)$ to $(L = n_T = n_R = 3)$, the BER strongly decreases (*e.g.*, from 10^{-4} to 10^{-7} for SNR $= 15$ dB), and the same is for the systems with $(L = n_T = n_R = 3)$ and $(L = n_T = n_R = 4)$ *e.g.*, the BER decreases from 10^{-5} to 10^{-7} for SNR $= 15$ dB. The gain offered by the $(L = n_T = n_R = 4)$ case with respect to the case with $(L = n_T = n_R = 2)$ is of the order of 9 dB. This simulation has been performed under the NLOS propagation scenario so, in principle, the diversity order should be high. Note that in NLOS the receiver well performs with respect to bandwidth efficient modulations since the possible phase rotation induced by reflections are not so critical in PPM modulation.

The absence of orthogonality among the matrix codewords provides a decrease of the diversity order with respect to the maximum one. Moreover, a reduction of the number of codewords may affect the BER at the cost of a transmission rate reduction. Under the above specifications, the rate of a $(L = n_T = n_R = 4)$ system is 6 times higher than the case of 2-PPM with single LED and photodiode.

In Fig. 5 we consider the effect of diversity for three different propagation scenarios *i.e.*, *pLOS*, *mLOS* and *NLOS*, referring to 0.2 m, 1 m and 3 m, respectively [15]. As anticipated, even if the channel coefficients are higher in the *pLOS*, this last does not exhibit high diversity order, while *NLOS* does. The *mLOS* case presents performance in between. More, even in the case of *pLOS* the matrix $\mathbf{H}$ is expected to be invertible since direct paths do not necessarily imply correlated fading. Specifically, the gain of *NLOS* is around 15 dB, compared to *pLOS*, while the gain offered in comparison with *mLOS* is up to 8 dB.

Furthermore, due to the important role of channel knowledge, we evaluated the channel robustness compared to an imperfect channel knowledge. We considered the term σ_h^2 related to the amplitude of channel $h(t)$. It is formally defined as

$$\sigma_h^2 = 1 - \frac{\int_T |\hat{h}(t)|^2 dt}{\int_T |h(t)|^2 dt}, \tag{17}$$

being $\hat{h}(t)$ the estimation of the channel. It includes not only the error in estimating the amplitudes but, more, the effect of signal misalignment, that is, synchronization. The main difference between the estimation and real channel is due to the ambient noise, and a value of $\sigma_h^2 = 60\%$ means that the noise power during the estimation process is 2 dB less the power received during the estimation phase. By fact, typical values for σ_h^2 are of the order of $0.01 \div 0.1$. In Fig. 6, when the channel estimation is very high (*i.e.*, $\sigma_h^2 \geq 40\%$) the

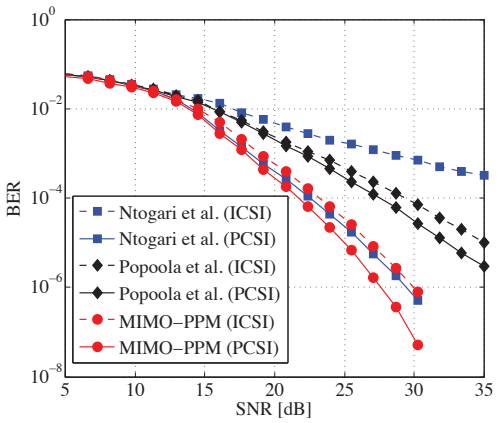

Fig. 7. Comparison of proposed scheme with the approaches pursued in [17] and [18].

receiver is unable to achieve reliable performance, while for estimation errors till to 30% the system achieves very good performance since the difference to ideal case (*i.e.*, $\sigma_h^2 = 0$) is negligible.

Finally, in Fig. 7 we show the comparison between the proposed scheme (labeled as "MIMO-PPM") and the contributions in [17] (labeled as "Ntogari et al.") and [18] (labeled as "Popoola et al."). For each scheme, two different curves are presented *i.e.*, (*i*) one related to the Perfect Channel State Information (PCSI) case, and (*ii*) one for the Imperfect Channel State Information (ICSI), which is referred to $\sigma_h^2 = 0.1\%$. Moreover, each curve represents the average BER obtained by considering different user positions in the room *i.e.*, at the room corner in $(1, 8, 1.5)$ where the propagation is $NLOS$, and at the room center $(5, 5, 1.5)$ where the propagation is $pLOS$.

While the scheme developed in [17] well performs when PCSI is available, it presents poor performance when ICSI is considered. On the other hand, the configuration characterized by four transmitting elements, and just one receiver in [18] is more robust with respect to channel state information, since the difference between PCSI and ICSI is limited to few dBs. Finally, the gain offered by the proposed MIMO-PPM scheme is sensible, especially at high SNRs, and the robustness is proved with respect to channel estimation error, as previously detailed.

V. Conclusion

In this paper we have described a novel technique for enhancing performance in indoor VLC systems. The proposed MIMO-LED PPM-based model aims to achieve a low BER and high data rate at the expense of higher hardware complexity, with limited computational cost given by simple matrix inversions, and is also robust with respect to channel estimation errors.

References

[1] D. C. O'Brien et al., "Indoor Visible Light Communications: challenges and prospects," *Proc of SPIE*, vol. 7091, 2008.

[2] M. Kavehrad, "Sustainable energy-efficient wireless applications using light," *IEEE Communications Magazine*, December 2010.

[3] T. Borogovac, M. Rahaim, and J. B. Carruhers, "Spotlighting for visible light communications and illumination," in *Workshop on Optical Communications, GLOBECOM*, 2010.

[4] D. Barros, S. Wilson, and J. Kahn, "Comparison of Orthogonal Frequency-Division Multiplexing and Pulse-Amplitude Modulation in Indoor Optical Wireless Links," *IEEE Trans. Comm.*, vol. 60, no. 1, pp. 153–163, 2012.

[5] J. Vucic et al., "513 Mbit/s Visible Light Communications Link Based on DMT-Modulation of a White LED," *Journal of Lightwave Technology*, vol. 28, no. 24, 2010.

[6] J. Vucic, C. Kottke, K. Habel, and K.-D. Langer, "803 Mbit/s Visible Light WDM Link based on DMT Modulation of a Single RGB LED Luminary," in *Optical Fiber Communication Conf. and Exposition (OFC/NFOEC) and the National Fiber Optic Engineers Conf.*, March 2011.

[7] *802.15.7 PHY and MAC Standard for Short Range Wireless Optical Communication Using Visible Light*, IEEE Std., 2010.

[8] L. Zeng et al., "High Data Rate MIMO Optical Wireless Communications Using White LED Lighting," *IEEE J. Sel. Areas Comm.*, vol. 27, 2009.

[9] R. M. R. Mesleh, H. Helgala and H.Haas, "Performance of optical spatial modulation with transmitters-receivers alignment," *IEEE Communication Letters*, vol. 15, no. 1, pp. 79–81, 2011.

[10] A. Vegni and M. Biagi, "An indoor localization algorithm in a small-cell led-based lighting system," in *Indoor Positioning and Indoor Navigation (IPIN), 2012 International Conference on*, 2012, pp. 1–7.

[11] M. Rahaim, T. Borogovac, and J. B. Carruthers, "CandLES: Communications and lighting emulation software," in *Proc. of the 5th ACM Intl. Workshop on Wireless Network Testbeds, Experimental Evaluation and Characterization*. ACM, 2010.

[12] J. R. Barry, *Wireless Infrared Communications*. Kluwer, 1994.

[13] R. Ramirez-Iniguez, S. M. Idrus, and Z. Sun, *Optical Wireless Communications*. CRC Press, 2008.

[14] J. M. Kahn and J. R. Barry, "Wireless Infrared Communications," *Proc. of the IEEE*, vol. 85, no. 2, pp. 265–298, February 1997.

[15] H. L. Minh et al., "100-Mb/s NRZ Visible Light Communications Using a Postequalized White LED," *IEEE Photonics Technology Letters*, vol. 21, no. 15, pp. 1063–1065, 2009.

[16] M. Biagi, A. M. Vegni, and T. D. Little, "LAT indoor MIMO-VLC —Localize, Access and Transmit—," in *Optical Wireless Communications (IWOW), 2012 International Workshop on*, oct. 2012, pp. 1 –3.

[17] G. Ntogari, T. Kamalakis, and T. Sphicopoulos, "Performance analysis of space time block coding techniques for indoor optical wireless systems," *Selected Areas in Communications, IEEE Journal on*, vol. 27, no. 9, pp. 1545 –1552, december 2009.

[18] W. Popoola, E. Poves, and H. Haas, "Spatial pulse position modulation for optical communications," *Lightwave Technology, Journal of*, vol. 30, no. 18, pp. 2948 –2954, sept.15, 2012.